Solution Behavior and X-ray Structure of Cationic Allylpalladium(II) Complexes with Iminophosphine Ligands. Kinetics and Mechanism of Allyl Amination by Secondary Amines

Bruno Crociani*,† and Simonetta Antonaroli

Dipartimento di Scienze e Tecnologie Chimiche, Università di Roma "Tor Vergata", 00133 Rome, Italy

Giuliano Bandoli

Dipartimento di Scienze Farmaceutiche, Università di Padova, Padua, Italy

Luciano Canovese,‡ Fabiano Visentin, and Paolo Uguagliati

Dipartimento di Chimica, Università di Venezia, Venice, Italy

Received October 14, 1998

Downloaded by CARLI CONSORTIUM on June 30, 2009
Published on February 27, 1999 on http://pubs.acs.org | doi: 10.1021/om980858l

The solution behavior of the cationic complexes [Pd(η^3-allyl)(P−N)]$^+$ (P−N = *o*-(PPh$_2$)C$_6$H$_4$-CH=NR (R = C$_6$H$_4$OMe-4, Me, CMe$_3$, (*R*)-bornyl); allyl = propenyl (**1a**−**4a**) and 3-methyl-2-butenyl (**1b**−**4b**)) consists essentially of three dynamic processes: (i) a very fast conformational change of the P−N chelate ring, which moves above and below the P−Pd−N coordination plane, (ii) a relatively fast $\eta^3-\eta^1-\eta^3$ interconversion which brings about a *syn*−*anti* exchange only for the allylic protons *cis* to phosphorus; (iii) a slower apparent rotation of the η^3-allyl ligand around its bond axis. For **1b**−**3b**, two geometrical isomers are observed, the predominant one having the allyl CMe$_2$ group *trans* to phosphorus. The complexes **4a** and **4b**, containing the chiral (*R*)-bornyl group, are present in solution with two and four diastereomeric species, respectively. The X-ray structural analysis of **4b**(ClO$_4$) shows the presence of two diastereomeric molecules in the unit cell, both having distorted-square-planar coordination geometries, characterized by rather elongated Pd−CMe$_2$ bonds *trans* to phosphorus and by a marked distortion of the allyl ligand, which is rotated away from the PPh$_2$ group. The complexes [Pd(η^3-allyl)(P−N)]$^+$ react with secondary amines HY in the presence of fumaronitrile, yielding [Pd(η^2-fn)(P−N)] and allylamines. Under pseudo-first-order conditions the amination rates obey the laws $k_{obs} = k_2[HY] + k_3[HY]^2$ for **1a**−**4a** and $k_{obs} = k_2[HY]$ for **1b**, **3b,** and **4b**. The k_2 term is related to direct bimolecular attack on a terminal allyl carbon of the substrate, whereas the k_3 term is ascribed to parallel attack by a further amine molecule on the intermediate [Pd(allyl)(P−N)(HY)]$^+$. The k_2 values increase with increasing basicity and decreasing steric hindrance of the amine, and with increasing electron-withdrawing ability and increasing bulkiness of the P−N nitrogen substituent. The higher amination rates for [Pd(η^3-allyl)(P−N)]$^+$, compared to [Pd(η^3-allyl)(α-diimine)]$^+$, are essentially due to lack of displacement equilibria of the P−N ligand by amines.

Introduction

In recent years the palladium-catalyzed amination of allyl substrates has been extensively studied for its relevance to organic synthesis.[1] Enantioselective allylic amination has been the subject of considerable interest, and several chiral ligands have been developed for this particular application.[2] Among these, diphosphines[3] and combined P,N donor[4] bidentate ligands have been used either in the reaction with [Pd(μ-Cl)(η^3-allyl)]$_2$ dimers or in the oxidative addition of allyl esters to palladium-(0) derivatives to generate *in situ* the catalyst (or catalyst precursor), which was generally assumed to be the cationic species [Pd(η^3-allyl)(L−L′)]$^+$. The cationic complexes with chiral P−N ligands [Pd(η^3-allyl)(P−N)]X (X$^-$ = SbF$_6^-$, PF$_6^-$, BF$_4^-$, CF$_3$SO$_3^-$) have been isolated, and their solution behavior has been studied by multinuclear and multidimensional NMR spectrometry in order to rationalize the observed high enantioselectivity (ee up to 97−99%) on the basis of (i) the relative concentrations of the configurational isomers resulting from different geometries of the allyl group, (ii) the rates of isomer interconversion, and (iii) the site and the

† E-mail: crociani@stc.uniroma2.it.
‡ E-mail: cano@unive.it.

(1) (a) Trost, B. M. *Angew. Chem., Int. Ed. Engl.* **1989**, *28*, 1173. (b) Godleski, S. A. In *Comprehensive Organic Synthesis*; Trost, B. M., Fleming, I., Semmelbach, M. F., Eds.; Pergamon: Oxford, U.K., 1991; Vol. 4, p 585. (c) Tsuji, J. *Palladium Reagents and Catalysts. Innovation in Organic Synthesis*; Wiley: Chichester, U.K., 1995; p 290.

(2) (a) Frost, C. G.; Howarth, J.; Williams, J. M. J. *Tetrahedron: Asymmetry* **1992**, *3*, 1089. (b) Williams, J. M. J. *Synlett* **1995**, 705. (c) Trost, B. M.; Van Vranken, D. L. *Chem. Rev.* **1996**, *96*, 395. (d) Tye, H.; Smyth, D.; Eldred, C.; Wills, M. *J. Chem. Soc., Chem. Commun.* **1997**, 1053.

10.1021/om980858l CCC: $18.00 © 1999 American Chemical Society
Publication on Web 02/27/1999

relative rates of nucleophilic attack at the nonequivalent terminal allyl carbons *trans* to donor atoms with different electronic and steric properties.[4c,d,5] To the best of our knowledge, however, no quantitative kinetic data for the allyl amination of $[Pd(\eta^3\text{-allyl})(P-N)]^+$ have been reported so far.

In previous papers we described the solution behavior of the complexes $[Pd(\eta^3\text{-allyl})(L-L')]^+$ (L−L′ = 2-(iminomethyl)pyridine[6] or 2-(thiomethyl)pyridine[7]), the kinetics of nucleophilic attack at the allyl group in these complexes by secondary and tertiary amines yielding zerovalent compounds $[Pd(\eta^2\text{-ol})(L-L')]$ in the presence of activated olefins (ol),[7,8] and the kinetics of oxidative allyl transfer from allylammonium cations to $[Pd(\eta^2\text{-ol})(L-L')]$ which regenerates the starting derivatives $[Pd(\eta^3\text{-allyl})(L-L')]^+$.[9] While the observed dynamic processes consist essentially of an apparent rotation of the η^3-allyl ligand around its bond axis to the metal and/or inversion at sulfur involving exchange of the two coordinating sulfur lone pairs for the 2-(thiomethyl)pyridine ligands, the kinetic data suggest the mechanism

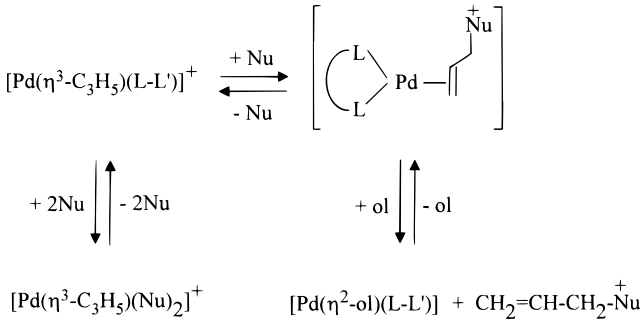

(Nu = secondary and tertiary amine; ol = activated olefin)

The nucleophilic attack occurs at a terminal allyl carbon of the cationic substrate at different rates, depending on the steric and electronic properties of L−L′ and Nu, and it is also accompanied by reversible displacement of the L−L′ ligand by the more coordinating amines.

We therefore decided to extend these studies to the cationic complexes $[Pd(\eta^3\text{-allyl})(P-N)]^+$ containing iminophosphine ligands of the (2-(diphenylphosphino)-benzylidene)amine type in order (i) to stabilize the complex toward displacement of the P−N chelate ligand by the entering amine and (ii) to investigate the influence of the coordinated PPh_2 unit on the reaction rates. As indicated by substitution reactions on palladium(0) adducts,[10] iminophosphines are better chelating ligands than 2-(iminomethyl)pyridines. On the other hand, it is well-known that the PPh_2 group in P−N ligands enhances the reactivity of the corresponding $(\eta^3$-allyl)-palladium(II) cationic complexes toward nucleophilic attack at the allyl moiety (and particularly at the terminal carbon *trans* to phosphorus), due to the better π-accepting properties and higher *trans* influence of the phosphino group relative to the N-donor group.[11]

In the present work, we have also used an asymmetrically substituted allyl ligand (namely, the 3-methyl-2-butenyl ligand) in order to gain a better understanding of the dynamic processes involving isomer interconversion for the cationic substrates $[Pd(\eta^3\text{-allyl})(P-N)]^+$ and of factors affecting the regiochemistry of allylic amination.

Results and Discussion

NMR Spectra and Solution Behavior. The ^1H and $^{31}P\{^1H\}$ NMR spectroscopic data for the η^3-propenyl complexes **1a**(BF_4)−**4a**(BF_4) and for the corresponding η^3-3-methyl-2-butenyl derivatives **1b**(BF_4)−**4b**(BF_4) are summarized in Table 1, while the $^{13}C\{^1H\}$ NMR results of some selected compounds are reported in Table 2. The configurations of the complexes are sketched in Scheme 1, along with the numbering scheme for the allylic protons and carbons.

For the η^3-3-methyl-2-butenyl derivatives, two *cis* and *trans* isomeric structures, **II** and **III**, are possible. However, due to the nonplanarity of the chelate six-membered ring of these complexes, as revealed by the X-ray structure of **4b**(ClO_4) (see further), the imino carbon and the *ortho*-disubstituted phenyl group of the P−N ligand lie on the same side out of the N−Pd−P coordination plane, whereas the nitrogen substituent R and one of the phenyl groups of the PPh_2 unit are in pseudoaxial positions on the opposite side of the N−Pd−P coordination plane. Such an asymmetric conformation of the chelate P−N ligand, compounded with the different orientations of the η^3-allyl group, increases to four the number of possible isomers for each configuration **I**−**III** as shown in Figure 1. The isomeric species **A** and

Downloaded by CARLI CONSORTIUM on June 30, 2009
Published on February 27, 1999 on http://pubs.acs.org | doi: 10.1021/om980858l

(3) (a) Hayashi, T.; Yamamoto, A.; Ito, Y. *Tetrahedron Lett.* **1988**, *29*, 99. (b) Hayashi, T.; Yamamoto, A.; Ito, Y.; Nishioka, E.; Miura, H.; Yanagi, K. *J. Am. Chem. Soc.* **1989**, *111*, 6301. (c) Hayashi, T.; Kishi, K.; Yamamoto, A.; Ito, Y. *Tetrahedron Lett.* **1990**, *31*, 1743. (d) Trost, B. M.; Van Vranken, D. L. *Angew. Chem., Int. Ed. Engl.* **1992**, *31*, 228. (e) Trost, B. M.; Van Vranken, D. L.; Bingel, C. *J. Am. Chem. Soc.* **1992**, *114*, 9327 (f) Trost, B. M.; Van Vranken, D. L. *J. Am. Chem. Soc.***1993**, *115*, 444. (g) Trost, B. M.; Bunt, R. C. *J. Am. Chem. Soc.* **1994**, *116*, 4089. (h) Trost, B. M.; Krueger, A. C.; Bunt, R. C.; Zambrano, J. *J. Am. Chem. Soc.* **1996**, *118*, 6520. (i) Mori, M.; Kuroda, S.; Zhang, C. S.; Sato, Y. *J. Org. Chem.* **1997**, *62*, 3263. (j) Uozumi, Y.; Tanahashi, A.; Hayashi, T. *J. Org. Chem.* **1993,** *58*, 6826. (k) Yamazaki, A.; Achiwa, K. *Tetrahedron: Asymmetry* **1995**, *6*, 1021. (l) Thorey, C.; Wilken, J.; Henin, F.; Martens, J.; Mehler, T.; Muzart, J. *Tetrahedron Lett.* **1995**, *36*, 5527. (m) Yamazaki, A.; Achiwa, I.; Achiwa, K. *Tetrahedron: Asymmetry* **1996**, *7*, 403.

(4) (a) von Matt, P.; Loiseleur, O.; Kock, G.; Pfaltz, A.; Lefeber, C.; Feucht, T.; Helmchen, G. *Tetrahedron: Asymmetry* **1994**, *5*, 573. (b) Jumnah, R.; Williams, A. C.; Williams, J. M. J. *Synlett* **1995**, 821. (c) Togni, A.; Burckhardt, U.; Gramlich, V.; Pregosin, P. S.; Salzmann, R. *J. Am. Chem. Soc.* **1996**, *118*, 1031. (d) Burckhardt, U.; Gramlich, V.; Hoffmann, P.; Nesper, R.; Pregosin, P. S.; Salzmann, R.; Togni, A. *Organometallics* **1996**, *15*, 3496. (e) Burckhardt, U.; Baumann, M.; Togni, A. *Tetrahedron: Asymmetry* **1997**, *8*, 155.

(5) (a) Sprinz, J.; Kiefer, M.; Helmchen, G.; Reggelin, M.; Huttner, G.; Walter, O.; Zsolnai, L. *Tetrahedron Lett.* **1994**, *35*, 1523. (b) Baltzer, N.; Macko, L.; Shaffner, S.; Zehnder, M. *Helv. Chim. Acta* **1996**, *79*, 803. (c) Fernàndez-Galan, R.; Jalòn, F. A.; Manzano, B. R.; Rodrìguez-de la Fuente, J.; Vrahami, M.; Jedlicka, B.; Weissensteiner, W.; Jogl, G. *Organometallics* **1997**, *16*, 3758.

(6) Crociani, B.; Antonaroli, S.; Paci, M.; Di Bianca, F.; Canovese, L. *Organometallics* **1997**, *16*, 384.

(7) (a) Canovese, L.; Visentin, F.; Uguagliati, P.; Chessa, G.; Lucchini, V.; Bandoli, G. *Inorg. Chim. Acta* **1998**, *275*, 385. (b) Canovese, L.; Visentin, F.; Uguagliati, P.; Chessa, G.; Pesce, A. *J. Organomet. Chem.* **1998**, *566*, 61.

(8) (a) Crociani, B.; Antonaroli, S.; Di Bianca, F.; Canovese, L.; Visentin, F.; Uguagliati, P. *J. Chem. Soc., Dalton Trans.* **1994**, 1145. (b) Canovese, L.; Visentin, F.; Uguagliati, P.; Di Bianca, F.; Antonaroli, S.; Crociani, B. *J. Chem. Soc., Dalton Trans.* **1994**, 3113. (c) Canovese, L.; Visentin, F.; Uguagliati, P.; Crociani, B.; Di Bianca, F. *Inorg. Chim. Acta* **1995**, *235*, 45.

(9) Canovese, L.; Visentin, F.; Uguagliati, P.; Di Bianca, F.; Fontana, A.; Crociani, B. *J. Organomet. Chem.* **1996**, *508*, 101.

(10) Antonaroli, S.; Crociani, B. *J. Organomet. Chem.* **1998**, *560*, 137.

(11) (a) Szabò, K. J. *Organometallics* **1996**, *15*, 1128 and references therein. (b) Oslob, J. D.; Åkermark, B.; Helquist, P.; Norrby, P. O. *Organometallics* **1997**, *16*, 3015 and references therein.

Table 1. Selected ^{1}H and ^{31}P{^{1}H} NMR Data[a]

		iminophosphine protons		allyl protons						
complex	isomer[b]	N=C*H*	other signals	H_{1s}	H_{1a}	H_2	H_{3s}	H_{3a}	CH_3	^{31}P resonance
1a(BF_4)	**I**	8.33 d (2.8)[c]	3.81s [OCH_3]	4.05 dd (7.0)[c] (7.0)[d]	3.65 dd (9.5)[c] (14.1)[d]	5.84 m	3.42 d(br) (6.0)[d]	2.95 d(br) (13.0)[d]		22.07 s
2a(BF_4)	**I**	8.48[e]	4.02[e] [NCH_3]	4.95 dd (6.7)[c] (6.7)[d]	3.98 dd (9.0)[c] (13.0)[d]	5.88 m	3.11 d(br) (8.4)[d]			
3a(BF_4)	**I**	8.50 s	1.23 s [C(CH_3)$_3$]	4.95 dd (6.9)[c] (6.9)[d]	3.78 dd (10.6)[c] (14.7)[d]	5.74 m	3.43 (br)	2.95 (br)		26.09 s
4a(BF_4)	**I**[f]	8.54 s	4.56 m(br) [NC*H*] 4.48 m(br) [NC*H*]	4.87 (br) 4.70 (br)	4.05 (br) 3.77 (br)	5.83 m	3.40 (br) 3.32 (br)	2.98 (br) 2.82 (br)		23.20 s
	I[f,g]	8.55 s 8.50 s	4.58 m [NC*H*] 4.45 m [NC*H*]	4.82 dd (6.0)[c] (6.0)[d] 4.66 dd (6.0)[c] (6.0)[d]	4.01 dd (10.0)[c] (13.5)[d] 3.68 dd (10.4)[c] (13.6)[d]	5.86 m	3.48 d(br) (5.0)[d] 3.35 d(br) (5.0)[d]	3.03 d(br) (12.2)[d] 2.80 d(br) (12.0)[d]		
1b(BF_4)	**II** (93%)	8.39 d (3.3)[c]	3.80 s [OCH_3]			5.28 t (10.0)[d]	3.12 (br)[h]	2.65 (br)[i]	0.96 d[j] (10.3)[c] 1.28 d[k] (5.9)[c]	25.02 s
	III (7%)	8.29 d (3.3)[c]	3.82 s [OCH_3]	mk[l]	3.70 dd (9.8)[c] (14.5)[d]	5.60 dd (8.2)[d] (14.5)[d]			0.92 d[j] (9.8)[c] 1.06 d[k] (6.2)[c]	20.37 s
2b(BF_4)	**II** (77%)	8.56[e]	3.81[e] [NCH_3]			5.40 t (10.0)[d]	2.77 (br)		2.07 d[j] (11.0)[c] 1.59 d[k] (6.0)[c]	23.50 s
	III (23%)	8.42[e]	4.01[e] [NCH_3]	4.72 dd (7.7)[c] (7.7)[d]	3.96 dd (10.0)[c] (13.9)[d]	5.62 dd			0.92 d[j] (8.2)[c] 1.11d[k] (6.0)[c]	19.07 s
3b(BF_4)	**II** (82%)	8.55 d (3.6)[c]	1.20 s [C(CH_3)$_3$]			5.23 t (9.7)[d]	2.75 (br)	2.50 (br)	2.04 d[j] (11.5)[c] 1.50d[k] (6.7)[c]	31.01 s
	III (18%)	8.49 d (4.9)[c]	1.26 s [C(CH_3)$_3$]	4.65 dd (7.9)[c] (7.9)[d]	3.68 dd (10.9)[c] (14.1)[d]	5.39 dd			0.98 d[j] (9.6)[c] 1.23 d[k] (6.6)[c]	24.87 s
4b(BF_4)	**II** (83%)[m]	8.55 s	4.36 m(br) [NC*H*]			5.26 m(br)	2.97 (br)	2.40 (br)	1.93 d[j] (10.05)[c] 1.54 d[k] (5.6)[c]	25.62 s
	III (17%)[f]	8.47 s	4.60 m [NC*H*] 4.58 m [NC*H*]	4.45 dd (7.5)[c] (7.5)[d] mk[n]	4.06 dd (10.0)[c] (15.0)[d] 3.57 dd (10.5)[c] (14.0)[d]	5.60 dd (7.6)[d] (15.0)[d] 5.47 dd (8.2)[d] (14.0)[d]			mk mk	21.29 s 20.32 s

[a] In $CDCl_3$ at 30 °C unless otherwise stated. Satisfactory integration values were obtained; coupling constants are given in Hz. Abbreviations: s, singlet; d, doublet; t, triplet; dd, doublet of doublets; m, multiplet, mk, masked. [b] See Scheme 1 for isomer structure and numbering scheme; the percentages of isomer **II** and **III** are given in parentheses. [c] *J*(PH). [d] *J*(HH). [e] Unresolved multiplet. [f] Two diastereoisomers in 1:1 molar ratio. [g] At −35 °C. [h] At −35 °C the signal is a doublet with *J*(HH) = 7.8 Hz. [i] At −35 °C the signal is a doublet with *J*(HH) = 14.6 Hz. [j] *syn* methyl group. [k] *anti* methyl group. [l] Masked by the signal at 3.80 ppm. [m] Two diastereoisomers in fast interconversion; at −40 °C the diastereoisomer ratio is *ca.* 4:1. [n] Masked by the signal at 4.36 ppm.

B′ (or **B** and **A′**) differ from each other in the opposite orientation of the allyl ligand relative to the rest of the molecule. If they are both present in solution, they should be observable in the NMR spectra, unless a fast interconversion occurs. For R = C_6H_4OMe-4, Me, and CMe_3, the isomers **B** and **B′** are the enantiomeric forms of **A** and **A′**, respectively, and they cannot be distinguished in the NMR spectra under the experimental conditions used in this study.

For the cationic complexes **1a**−**3a**, all having configuration **I**, the ^{1}H NMR spectra are characterized by a single set of proton resonances even at the lowest temperature explored (−75 °C, in CD_2Cl_2). A single set of ^{31}P and ^{13}C resonances is also observed at 30 °C. These data appear to indicate either the presence of only one pair of enantiomers **A**/**B** (or **A′**/**B′**) or the occurrence of fast interconversion processes involving the four isomers.

Downloaded by CARLI CONSORTIUM on June 30, 2009
Published on February 27, 1999 on http://pubs.acs.org | doi: 10.1021/om980858l

Table 2. Selected $^{13}C\{^1H\}$ NMR Data[a]

		iminophosphine carbons		allyl carbons			
complex	isomer[b]	N=CH	other signals	C_1[c]	C_2	C_3[d]	CH_3
1a(BF_4)	**I**	174.98	55.65 [O*C*H$_3$]	85.54 d (27.4)	123.11	56.10	
3a(BF_4)	**I**	166.06 d (5.9)	29.76 [C(*C*H$_3$)$_3$]	80.79 d (30.4)	120.85 d (6.5)	56.19	
1b(BF_4)	**II**	167.35 d (4.7)	55.60 [O*C*H$_3$]	122.81 d (25.4)	111.47 d (5.2)	45.98	25.35, 20.72 d (4.9)
2b(BF_4)	**II**	168.72 d (6.2)	53.02 [N*C*H$_3$]	118.93 d (26.7)	111.69 d (5.7)	46.10 d (4.5)	26.92, 20.61 d (5.3)
	III	168.53 d (3.7)	59.81 [N*C*H$_3$]	73.54 d (28.8)	118.37 d (6.0)	86.99 d (6.6)	25.59, 20.92
3b(BF_4)	**II**	166.30 d (5.1)	30.08 [C(*C*H$_3$)$_3$]	mk[e]	110.06 d (6.8)	40.39	28.60, 21.58 d (5.0)
	III	167.26 d (5.1)	29.91 [C(*C*H$_3$)$_3$]	71.60 d (30.6)	115.51 d (6.5)	88.80	26.22, 21.69

[a] In $CDCl_3$ at 30 °C; *J*(PC) coupling constants (Hz) in parentheses. [b] See Scheme 1 for isomer structure and numbering scheme. [c] *trans* to phosphorus. [d] *cis* to phosphorus. [e] Masked by the phenyl carbon resonances in the range 125−130 ppm.

Scheme 1[a]

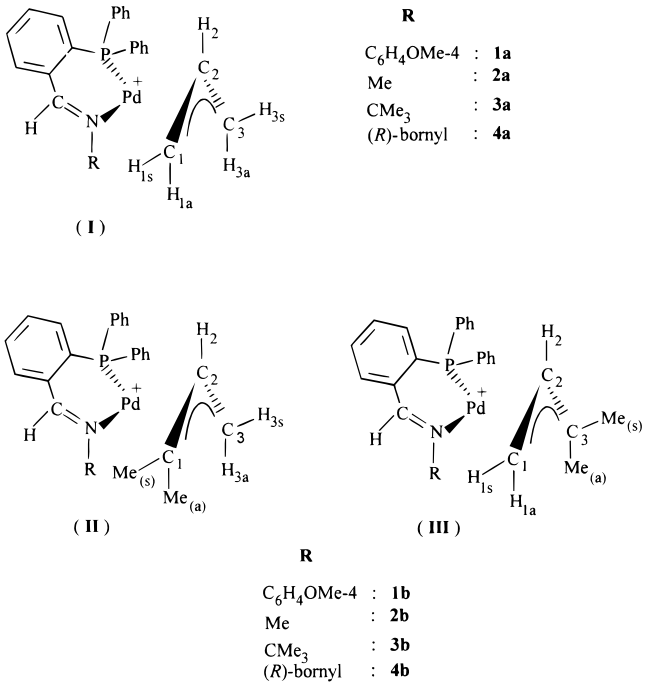

[a] (*R*)-Bornyl = *endo*-(1*R*)-1,7,7-trimethylbicyclo[2.2.1]hept-2-yl.

For the **1b**−**3b** derivatives, both *cis* and *trans* isomers of configurations **II** and **III** are detected in solution (the isomer **II** being in any case predominant). Each geometrical isomer is characterized by a single set of proton resonances in the temperature range from −35 to 30 °C in $CDCl_3$, even though it may be present in solution with four isomers, namely the two enantiomeric pairs **A**, **B** and **A′**, **B′** of Figure 1. A single set of phosphorus and carbon resonances is also observed for each geometrical isomer at 30 °C.

The assignment of the allyl resonances and of the configurations **II** and **III** to the *cis* and *trans* isomers of complexes **1b**−**4b** is based essentially on the differences in *J*(HH) values between the allylic protons and on the differences in *J*(PH) and *J*(PC) values between phosphorus and allylic protons and carbons. It is well-documented that in allyl complexes with phosphine ligands, the ^{31}P nucleus gives larger coupling constants with ^1H and ^{13}C nuclei in *trans* positions.[5b,5c,12] For complex **2b**, the above assignments are confirmed by the interligand and intraligand NOEs observed for isomers **II** and **III** in a 2D ^1H NMR ROESY experiment carried out on their equilibrium mixture in $CDCl_3$ (Table 3). For each isomer **II** and **III**, the allylic methyl protons exhibit long-range coupling constants of different magnitudes with phosphorus. According to intraligand NOEs, in both isomers **II** and **III** of complex **2b** the *syn* methyl protons are characterized by larger *J*(PH) values than the corresponding *anti* methyl protons. Consequently the related signals in the complexes containing the η^3-3-methyl-2-butenyl ligand were assigned on the basis of the observed difference in the *J*(PH) values.

The variable-temperature spectra and the phase-sensitive 2D ROESY spectrum of **2b** suggest that the cationic complexes are fluxional in solution. Two dynamic processes are observed: a relatively fast *syn*−*anti* exchange of the H_{3s} and H_{3a} protons *cis* to phosphorus and a slower P−N ligand site exchange (which may also be viewed as a 180° rotation of the allyl ligand around its bond axis to palladium). As can be seen in Table 1, at 30 °C the H_{3s} and H_{3a} protons of complexes **1a**−**4a** and of isomers **II** of **1b**−**4b** are generally detected as two broad signals, which coalesce into a single broad resonance for **2a** and for isomer **II** of **2b**. The fine structure of these signals can be observed at lower temperature (*cf.* the spectra of **4a** and **1b** at −35 °C). The $H_{3s} \leftrightarrow H_{3a}$ exchange may be explained in terms of a selective $\eta^3-\eta^1-\eta^3$ interconversion of the allyl ligand, which involves initial breaking of the Pd−C_1 bond (*trans* to P), rotation around the C_2-C_3 bond in the η^1-allyl transient, and re-formation of the η^3 complex with interchange of H_{3s} and H_{3a} protons. Such $\eta^3-\eta^1-\eta^3$ interconversion has also been observed for other (η^3-allyl)palladium(II) complexes with bidentate P−N,[5a,c] P−P,[13] P−S,[14] and P−O[15] ligands. However, for the isomers of type **III** (where the allyl terminus *cis* to phosphorus is the CMe_2 moiety) no *syn*−*anti* exchange of either the H_{1s} and H_{1a} protons or the $Me_{(s)}$ and $Me_{(a)}$ protons takes place at an appreciable rate, as shown

(12) (a) Powell, J.; Shaw, B. L. *J. Chem. Soc. A* **1967**, 1839. (b) Åkermark, B.; Krakenberger, B.; Hansson, S.; Vitagliano, A. *Organometallics* **1987**, *6*, 620.

Downloaded by CARLI CONSORTIUM on June 30, 2009
Published on February 27, 1999 on http://pubs.acs.org | doi: 10.1021/om980858l

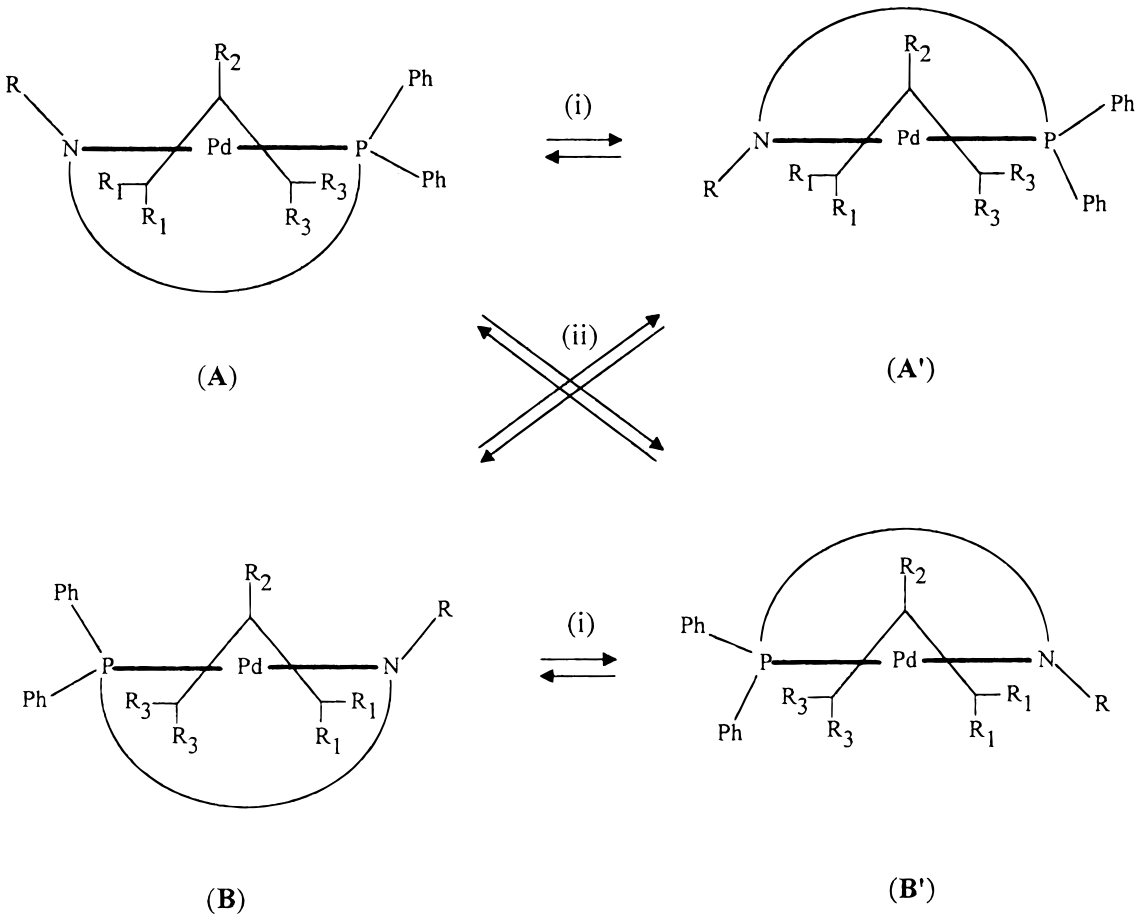

$R_1 = R_2 = R_3 = H$: **I**
$R_1 = Me$; $R_2 = R_3 = H$: **II**
$R_1 = R_2 = H$; $R_3 = Me$: **III**

Figure 1. Side view from the allyl ligand toward the Pd atom for the four possible isomers of each configuration **I**−**III**. The curved line represents the $=CHC_6H_4-$ unit lying above or below the N−Pd−P plane. Legend: (i) interconversion through a conformational change of the chelate P−N ligand (see text); (ii) interconversion through a selective $\eta^3-\eta^1-\eta^3$ rearrangement of the allyl ligand (see text).

Table 3. Selected 2D ^{1}H Data[a] for 2b(BF_4)

isomer	intraligand NOEs	interligand NOEs
II	N=CH [8.56]···NMe [3.81]	NMe [3.81]···$Me_{(s)}$ [2.07]
	H_2 [5.40]···$Me_{(s)}$ [2.07] (11.0)[b]	NMe [3.81]···$Me_{(a)}$ [1.59]
	$H_{3a} + H_{3s}$ [2.77]··· $Me_{(a)}$ [1.59] (6.0)[b]	
	$Me_{(a)}$ [1.59]···$Me_{(s)}$ [2.07]	
III	N=CH [8.42]···NMe [4.01]	NMe [4.01]···H_{1s} [4.72]
	H_2 [5.62]···H_{1s} [4.72]	NMe [4.01]···H_{1a} [3.96]
	H_2 [5.62]···$Me_{(s)}$ [0.92] (8.2)[b]	
	H_{1a} [3.96]···$Me_{(a)}$ [1.11] (6.0)[b]	
	$Me_{(a)}$ [1.11]···$Me_{(s)}$ [0.92]	

[a] Values in brackets are the proton chemical shifts in ppm. [b] J(PH).

by the absence of exchange cross-peaks between the H_{1s} and H_{1a} signals and between the $Me_{(s)}$ and $Me_{(a)}$ signals of isomer **III** in the phase-sensitive 2D ROESY spectrum of **2b** (see Figure 2 for the methyl signal region).

On the other hand, the observation of exchange cross-peaks between the signals of isomer **II** and the corresponding signals of isomer **III** in the latter spectrum (see Figure 2 for $Me_{(s)}$ and $Me_{(a)}$ signals) clearly indicates that the isomers interconvert into each other through a dynamic process which involves a P−N ligand site exchange. Although no quantitative measurement was carried out, the sharpness of the interconverting signals points to a reduced rate for this process if compared to the marked broadening of the signals caused by the faster *syn*−*anti* exchange occurring simultaneously for isomer **II**.

In a consideration of the four possible isomers of Figure 1, the selective $\eta^3-\eta^1-\eta^3$ process brings about the **A** ↔ **B**′ and **A**′ ↔ **B** interconversions for the cationic complexes **1a**−**3a** and **1b**−**3b** of configurations **I** and **II,** respectively, while the P−N ligand site exchange brings about the same type of interconversion for complexes **1a**−**3a** and the **II** ↔ **III** interconversion for

(13) (a) Breutel, C.; Pregosin, P. S.; Salzmann, R.; Togni, A. *J. Am. Chem. Soc.* **1994**, *116*, 4067. (b) Pregosin P. S.; Salzmann, R.; Togni, A. *Organometallics* **1995**, *14*, 842. (c) Barbaro, P.; Pregosin P. S.; Salzmann, R.; Albinati, A.; Kunz, R. W. *Organometallics* **1995**, *14*, 5160. (d) Pregosin, P. S.; Salzmann, R. *Coord. Chem. Rev.* **1996**, *155*, 35.

(14) Hermann, J.; Pregosin, P. S.; Salzmann, R.; Albinati, A. *Organometallics* **1995**, *14*, 3311.

(15) Hosokawa, T.; Wakabayashi, Y.; Hosokawa, K.; Tsuji, T.; Murabashi, S. I. *J. Chem. Soc., Chem. Commun.* **1996**, 859.

Downloaded by CARLI CONSORTIUM on June 30, 2009
Published on February 27, 1999 on http://pubs.acs.org | doi: 10.1021/om980858l

Downloaded by CARLI CONSORTIUM on June 30, 2009
Published on February 27, 1999 on http://pubs.acs.org | doi: 10.1021/om980858l

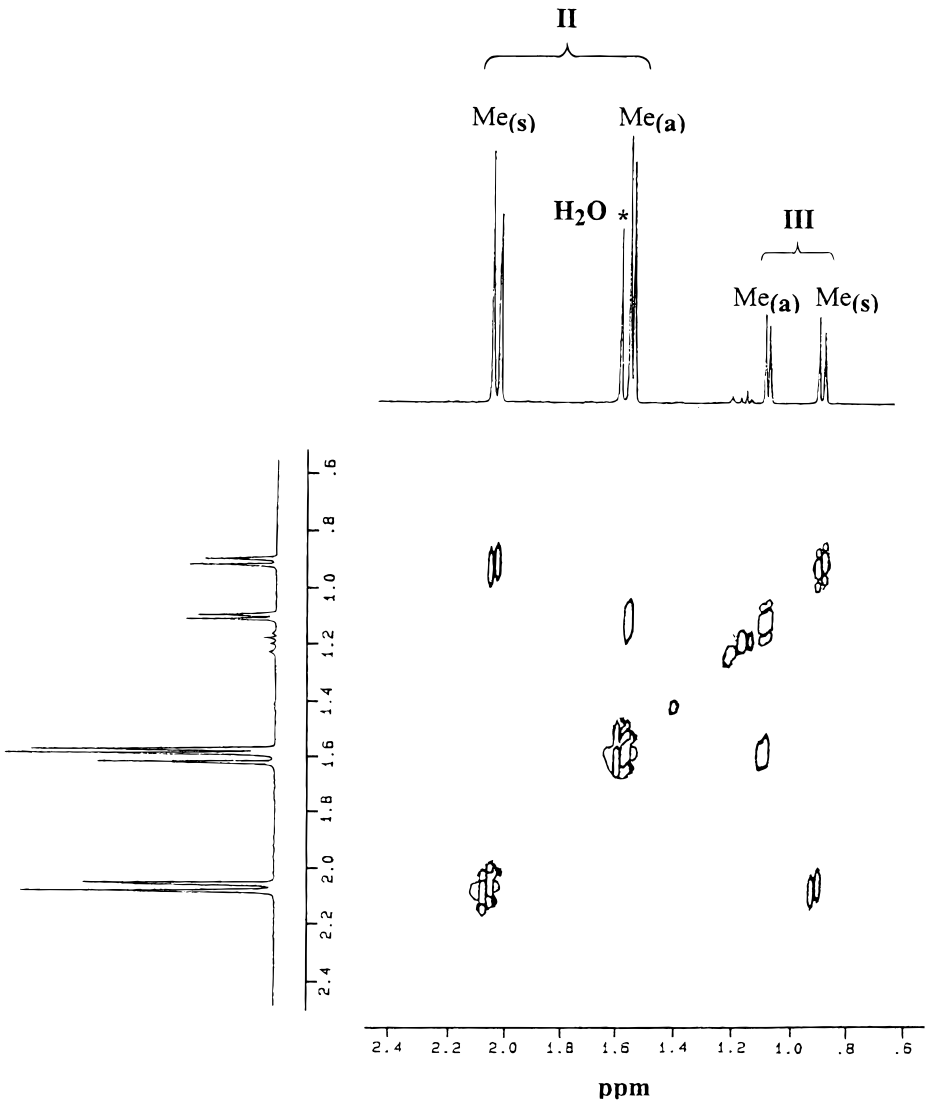

Figure 2. Phase-sensitive 2D ^{1}H ROESY spectrum of **2b**(BF_4) in the region of the allylic methyl signals, in $CDCl_3$ at 30 °C. Only positive NOEs are shown.

1b−**3b**. Preliminary crystallographic data on **1a(**BF_4) have shown that in the solid state the complex is formed by an equimolar mixture of the isomeric species **B** and **A′**.[16] The failure to detect such isomers (or those of types **B′** and **A**) in the ^{1}H NMR spectra of **1a** and of the other cationic complexes at low temperature (when the above dynamic processes are frozen) is very likely due to a low-energy conformational change of the chelate P−N ligand whereby a fast **A** ↔ **A′** (and **B** ↔ **B′**) interconversion takes place. Such a process, involving partial rotations of the PPh_2 unit (around the bonds of phosphorus with palladium and with the carbon atom of the *ortho*-disubstituted phenyl group) and of the N−R moiety (around the Pd−N bond), has been proposed to account for the fluxional behavior of the complexes [RhCl(CO)(P−N)][17] and [PdMe(OR)(P−N)],[18] containing a puckered six-membered chelate ring with *o*-(diphenylphosphino)-*N*,*N*-dimethylbenzylamine as the P−N ligand.

The solution behavior of complexes **4a** and **4b**, containing a chiral (*R*)-bornyl group, can be well-understood by taking into account the observed dynamic processes. For **4a** at −35 °C, the proton resonances are split into two sets of signals of *ca*. 1:1 relative intensity, indicating the presence of two diastereomeric species **A** (rapidly interconverting with **A′**) and **B** (rapidly interconverting with **B′**). As the temperature is raised, a progressive line broadening is observed and eventually at 30 °C some resonances coalesce into a single signal (*cf*. the imino proton at 8.54 ppm) because of the increasing rate of **A** ↔ **B′** and **B** ↔ **A′** interconversion mainly through the $\eta^3-\eta^1-\eta^3$ mechanism.

For **4b** at −40 °C, two diastereomeric species (*ca*. 4:1 molar ratio) of the major isomer **II** and two diastereomeric species (*ca*. 1:1 molar ratio) of the minor isomer **III** are observed. At 30 °C, the diastereomeric species of isomer **II** interconvert so rapidly as to give rise to broad time-averaged ^{1}H NMR signals, whereas the diastereomeric species of isomer **III** are characterized by fairly sharp resonances, which suggest a rather low rate of interchange. Consistently, the ^{31}P NMR spectrum at 30 °C shows an intense singlet for the rapidly interconverting diastereomeric species of isomer **II** and two 1:1 singlets of lower intensity for the diastereomeric

(16) Bandoli, G.; Crociani, B., preliminary results.
(17) Rauchfuss, T. B.; Patino, F. T.; Roundhill, D. M. *Inorg. Chem.* **1975**, *14*, 652.
(18) Kapteijn, G. M.; Spee, M. P. R.; Grove, D. M.; Kooijman, H.; Spek, A.; van Koten, G. *Organometallics* **1996**, *15*, 1405.

Table 4. Selected Bond Distances (Å) and Angles (deg) for 4b(ClO_4)

	molecule **A**	molecule **B**
Pd−P(1)	2.257(4)	2.248(4)
Pd−N(1)	2.16(1)	2.13(1)
Pd−C(8)	2.08(1)	2.11(2)
Pd−C(9)	2.14(2)	2.20(1)
Pd−C(10)	2.43(2)	2.39(2)
N(1)−C(7)	1.26(2)	1.27(2)
C(8)−C(9)	1.42(2)	1.49(2)
C(9)−C(10)	1.36(2)	1.38(2)
P(1)−Pd−N(1)	87.1(3)	88.9(3)
Pd−C(8)−C(9)	72.8(9)	73.1(9)
Pd−C(9)−C(10)	84.8(9)	80.1(9)
Pd−N(1)−C(7)	125.4(9)	126.9(9)
Pd−P(1)−C(1)	104.0(4)	106.5(4)
N(1)−C(7)−C(6)	127(1)	128(1)
P(1)−Pd−C(10)	161.9(4)	160.7(4)
N(1)−Pd−C(8)	168.2(5)	170.8(6)
C(8)−Pd−C(10)	64.3(6)	68.5(6)

species of isomer **III**. According to the 2D ^1H NMR data for **2b**, which rule out any $\eta^3-\eta^1-\eta^3$ process for isomer **III**, the diastereoisomers **III** of **4b** may interconvert through a sequence of a slow P−N ligand site exchange (**III**(**A** or **A′**) ↔ **II**(**B′** or **B**)), followed by a fast $\eta^3-\eta^1-\eta^3$ rearrangement (**II**(**B′** or **B**) ↔ **II**(**A** or **A′**)), and finally by another slow P−N ligand site exchange (**II**(**A** or **A′**) ↔ **III**(**B′** or **B**)). The above rearrangements (starting from isomer **II**) would also explain the presence of isomers **III** in the equilibrium mixture in solution, even though isomers **III** are not detected in the solid state, as revealed by the X-ray structural analysis of **4b**.

X-ray Structure of 4b(ClO_4). The solid-state structure of the (*R*)-bornyl complex **4b** was determined by X-ray diffraction. For this study, the perchlorate salt was chosen because the ClO_4^- anion is generally less affected by thermal disorder than BF_4^-. Some selected bond distances and angles are listed in Table 4. An ORTEP plot of the asymmetric unit cell is reported in Figure 3. There are two independent molecules in the cell, which are not superimposable, as can be seen in Figure 4, where superimposition of the (*R*)-bornyl groups brings about a nearly specular arrangement of the central metals and the coordinated ligands. Both molecules, however, have the same coordination geometry with the CMe_2 allyl terminus *trans* to phosphorus (structure **II** of Scheme 1) and the same orientation of the allyl ligand relative to the N−Pd−P coordination plane, with the central allyl carbon C(9) pointing out of this plane on the same side as the (*R*)-bornyl and the pseudoaxial P−Ph groups. The planar ring of the *ortho*-disubstituted phenyl group lies out of the N−Pd−P coordination plane, on the opposite side relative to the central allyl carbon C(9). The two molecules are therefore the diastereoisomers **A** and **B** of Figure 1. Thus, in the solid state the complex **4b** is present as an equimolar mixture of diastereoisomers **A** and **B**, with configuration **II**, whereas in $CDCl_3$ solution it is present as a mixture of both geometrical isomers **II** and **III** in a **II**/**III** molar ratio of *ca.* 4.9:1. At variance with the solid state, the two diastereomeric species of isomer **II**, detected in solution at −40 °C, are in a 4:1 rather than in a 1:1 molar ratio.

If one considers the inner coordination sphere as formed by the P- and N-donor atoms of the iminophosphine and by the terminal allyl carbons C(8) and C(10), the coordination geometry around the metal center is distorted square planar, with the allyl ligand markedly rotated away from the PPh_2 group, as can be seen in the side views of the molecules from the allyl ligand toward the Pd atom:

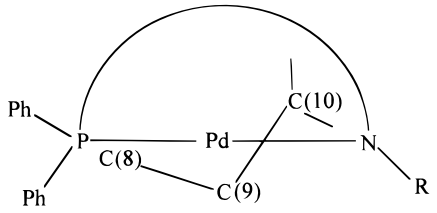

(molecule **A**)

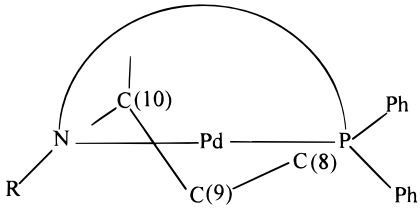

(molecule **B**)

The C(8) and C(9) atoms are both below the N−Pd−P plane (0.12 and 0.44 Å in **A**; 0.17 and 0.38 Å in **B**), whereas the C(10) atom lies above such a plane (0.53 Å in **A**; 0.54 Å in **B**). Similar rotation of the allyl moiety with respect to its idealized position has also been observed in related cationic complexes with P−N chelating ligands, containing the sterically demanding η^3-1,3-diphenylallyl fragment.[4c,d,5b]

The *ortho*-disubstituted phenyl ring plane (C(1)−C(6)) makes a dihedral angle of 54.4° (**A**) and 51.1° (**B**) with the N−Pd−P coordination plane, while the allyl plane (C(8)−C(9)-C(10)) makes a dihedral angle of 103.0° (**A**) and 114.0° (**B**) with the same plane. The allyl ligand is asymmetrically bound to the metal, as indicated by the Pd−C(10) bond (*trans* to P) being markedly longer than the Pd−C(8) bond (*trans* to N), in agreement with the higher *trans* influence of the phosphorus donor atom. The bond lengths and angles in the coordination sphere are in line with literature data for analogous [Pd(η^3-allyl)(P−N)]$^+$ complexes, with the outstanding exception of the Pd−C(10) bonds (2.43 Å (**A**) and 2.39 Å (**B**)) which are significantly longer than the reported Pd−C allyl bond lengths *trans* to phosphorus (2.216−2.268 Å).[4c,d,5b,c] We ascribe such lengthening and the marked rotation of the allyl group in **4b** to the steric repulsion between the allyl CMe_2 terminus and the bulky (*R*)-bornyl group. On the other hand, the marked asymmetry of the allyl group in the molecules **A** and **B** of complex **4b** may also be interpreted on the basis of a prevailing ene-yl coordination of this ligand, with the double bond *trans* to the phosphorus atom. This view is consistent with the long Pd−C(10) bond distances (2.43 and 2.39 Å in **A** and **B**, respectively) and also with the observed differences in the carbon−carbon bond lengths of the allylic unit (see Table 4).[29]

Kinetic Studies

The η^3-propenyl complexes **1a**−**4a** react smoothly with an excess of the secondary amines HY in $CHCl_3$

Downloaded by CARLI CONSORTIUM on June 30, 2009
Published on February 27, 1999 on http://pubs.acs.org | doi: 10.1021/om980858l

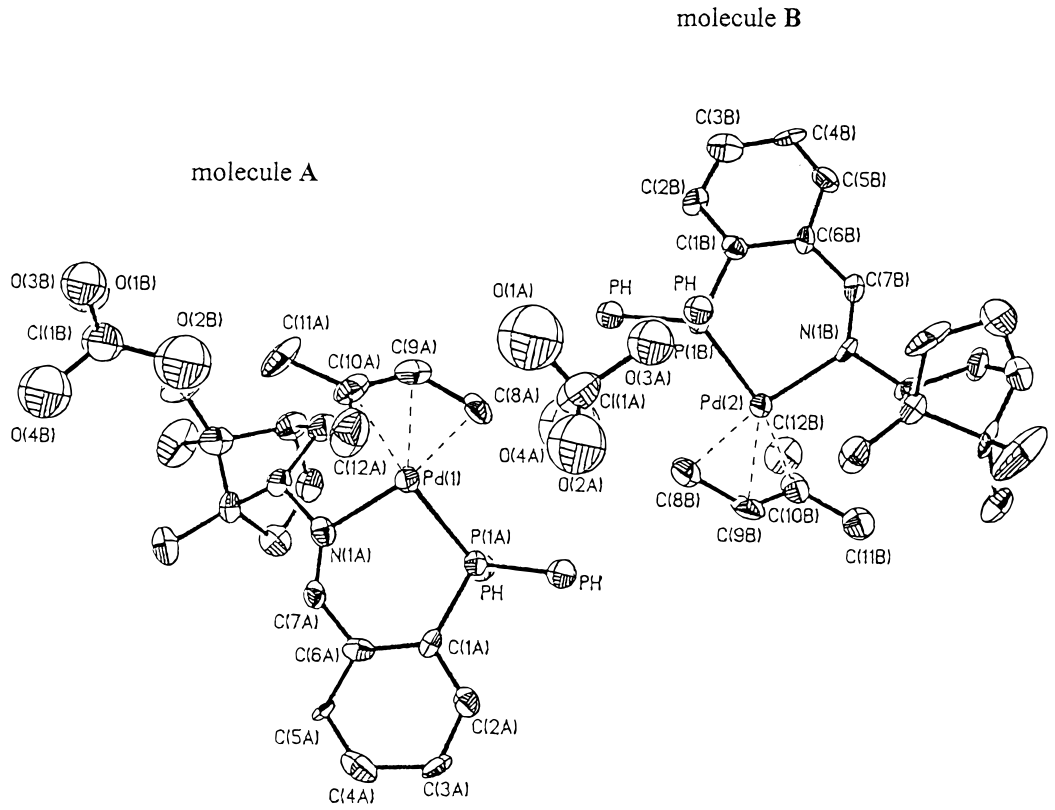

Figure 3. ORTEP view of the unit cell of **4b**(BF_4), with the two independent molecules **A** and **B**. The phenyl rings of the PPh_2 group have been indicated as PH for clarity.

at 25 °C in the presence of fumaronitrile (fn) to give the zerovalent complexes [Pd(η^2-fn)(P−N)] [10] and the corresponding allylamine (eq 1; HY = piperidine, diethylamine, morpholine).

$$[Pd(\eta^3\text{-}C_3H_5)(P{-}N)]^+ + HY_{(exc)} \xrightarrow[-H_2Y^+]{+fn_{(exc)}} [Pd(\eta^2\text{-fn})(P{-}N)] + CH_2{=}CHCH_2Y \quad (1)$$

1a−**4a**

Under the same experimental conditions, the reactions of the η^3-3-methyl-2-butenyl derivatives **1b**, **3b**, and **4b** involve either nucleophilic attack at the allyl termini (eq 2a; HY = diisopropylamine, diethylamine, piperidine) and/or deprotonation of the allyl ligand to isoprene (eq 2b), depending on the steric requirements of the amine.

$$[Pd(\eta^3\text{-}1,1Me_2C_3H_3(P{-}N)]^+ + HY_{(exc.)} \xrightarrow[-H_2Y^+]{+fn_{(exc.)}} \begin{cases} [Pd(\eta^2\text{-fn})(P{-}N)] + Me_2C{=}CH{-}CH_2Y + CH_2{=}CH{-}CMe_2Y & (2a) \\ [Pd(\eta^2\text{-fn})(P{-}N)] + CH_2{=}CH{-}CMe{=}CH_2 & (2b) \end{cases}$$

1b,**3b**,**4b**

According to ^{1}H NMR spectra recorded at different times for cationic complex/fn/HY reaction mixtures in a 1:1.2:5 molar ratio in $CDCl_3$ at 25 °C (with an initial complex concentration of 2.5×10^{-2} mol dm^{-3}), the reactions with the bulkier diisopropylamine are slow and proceed predominantly through eq 2b, whereas those with diethylamine are much faster and go to completion

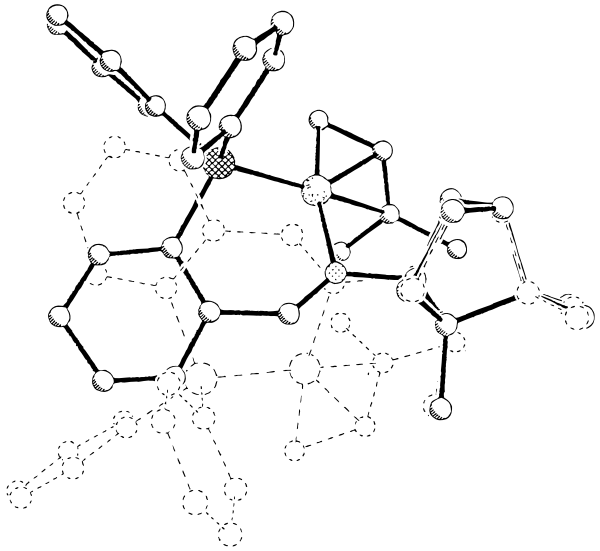

Figure 4. Superposition of the (*R*)-bornyl groups of molecule **A** (bold line) and molecule **B** (dotted line) for the cation **4b**.

essentially through eq 2a. In the latter case, the organic products consist of the allylamine $Me_2C{=}CHCH_2NEt_2$, resulting from attack at the less substituted allyl carbon, and a small amount of isoprene (2−5%). The reactions with the less sterically demanding piperidine are very fast and proceed exclusively through eq 2a. In this case, however, a mixture of the regioisomeric allylamines $Me_2C{=}CHCH_2Y$ and $CH_2{=}CHCMe_2Y$ is obtained.

The molar ratio $Me_2C{=}CHCH_2Y/CH_2{=}CHCMe_2Y$ appears to be kinetically controlled, as it depends not only on the different rates of nucleophilic attack at the

Downloaded by CARLI CONSORTIUM on June 30, 2009
Published on February 27, 1999 on http://pubs.acs.org | doi: 10.1021/om980858l

Downloaded by CARLI CONSORTIUM on June 30, 2009
Published on February 27, 1999 on http://pubs.acs.org | doi: 10.1021/om980858l

different allylic termini of the η^3-3-methyl-2-butenyl group but also on the subsequent isomerization process $CH_2{=}CHCMe_2Y \rightarrow Me_2C{=}CHCH_2Y$, the rate of which decreases with increasing concentration of fumaronitrile and with decreasing temperature. This is clearly shown by the results of reaction 2a for complex **3b** under different experimental conditions. When the reactants are mixed in **3b**/fn/piperidine ratios of 1:1.2:5 and 1:10:5 at 25 °C, the $Me_2C{=}CHCH_2Y/CH_2{=}CHCMe_2Y$ ratios (measured after 30 min, when the reaction is complete) are 2:1 and 1:1, respectively. When the same reactants are mixed in a 1:5:5 ratio at −30 °C, the observed $Me_2C{=}CHCH_2Y/CH_2{=}CHCMe_2Y$ ratio is 1:5 and remains constant throughout the reaction.

Similar reactions involving deprotonation of η^3-bound allyl ligands or isomerization of allylamines have been previously observed in the amination of various η^3-allylpalladium complexes.[19]

From the ^{1}H NMR studies of reactions 1 and 2a the following features are also apparent: (i) the rate of the $\eta^3{-}\eta^1{-}\eta^3$ process for complexes **1a**−**4a** and for isomer **II** of complexes **1b**, **3b**, and **4b** is greatly increased in the presence of the amine HY; (ii) the **II**/**III** molar ratio is not affected by the amine and remains constant throughout the reaction, whereas the **II** ↔ **III** interconversion rate is slightly increased in the presence of the amine; (iii) the chelate P−N ligand is not displaced by the entering amine.

For quantitative kinetic measurements the course of reactions 1 and 2a was followed by monitoring UV/vis spectral changes (λ, 500−200 nm) of $CHCl_3$ solutions of the complexes ($[Pd]_0 = 1 \times 10^{-4}$ mol dm^{-3}) in the presence of fn ($(2{-}8) \times 10^{-4}$ mol dm^{-3}) upon addition of variable aliquots of excess HY (1×10^{-3}−0.1 mol dm^{-3}). Under such pseudo-first-order conditions the reactions went smoothly to completion, as indicated by comparison of solution spectra after 7−8 half-lives with those of the final products independently prepared.[10] The conversion to the zerovalent [Pd(η^2-fn)(P−N)] complexes appears to obey the customary monoexponential absorbance (A) vs time (t) relationship $A_t = A_\infty + (A_0 - A_\infty)\exp(-k_{obs}t)$. The pseudo-first-order rate constants k_{obs} were determined by nonlinear regression of absorbance A_t data to time. No dependence of the rates on the fumaronitrile concentration could be detected in the range investigated. For reaction 1 the k_{obs} values fit the two-term second- and third-order rate law

$$k_{obs} = k_2\,[HY] + k_3[HY]^2 \qquad (3)$$

whereas for reaction 2a only the second-order term is observed:

$$k_{obs} = k_2[HY] \qquad (4)$$

The values of constants k_2 and k_3 are listed in Table 5.

The presence of the third-order term k_3 in the rate law, observed for the reaction of [Pd(η^3-allyl)(L−L′)]$^+$ (L−L′ = 2-(iminomethyl)pyridine) with secondary amines HY, was initially interpreted as resulting from a bimolecular attack by a hydrogen-bonded amine dimer in equilibrium with the monomer under the prevailing solvent, temperature, and concentration conditions.[8] On the other hand, the third-order rate law, observed for the amination of [PdCl(η^3-3-methyl-2-butenyl)(PPh_3)] with Me_2NH, was ascribed to a slow deprotonation of the intermediate formed in the rapid initial attack of the amine on the allyl ligand.[20] Since such a third-order term is absent in rate law (4) and in that observed in the reaction of [Pd(η^3-allyl)(L−L′)]$^+$ (L−L′ = 2-(thiomethyl)pyridine) with the same amines HY under the same conditions,[7] the above interpretations are to be ruled out and an alternative mechanism is to be devised.

Table 5. Rate Constants k_2 and k_3 for Reactions 1 and 2a in $CHCl_3$ at 25 °C

complex	amine[a]	k_2 (mol^{-1}dm^3 s^{-1})	k_3[b] (mol^{-2} dm^6 s^{-1})
1a	pip	1.9 ± 0.1	72 ± 22
	dea	0.21 ± 0.02	3.4 ± 1
	morph	0.23 ± 0.02	12 ± 3
2a	pip	0.45 ± 0.02	9 ± 2
	dea	0.032 ± 0.004	0.5 ± 0.1
3a	pip	3.4 ± 0.1	39 ± 15
	dea	0.29 ± 0.02	3 ± 1
4a	pip	3.9 ± 0.2	93 ± 23
	dea	0.40 ± 0.04	4.2 ± 1
1b	pip	0.031 ± 0.001	
	dea	0.0018 ± 0.0005	
3b	pip	0.116 ± 0.003	
	dea	0.011 ± 0.001	
4b	pip	0.076 ± 0.002	
	dea	0.0076 ± 0.0002	

[a] Abbreviations: Pip, piperidine; dea, diethylamine; morph, morpholine. [b] $k_3 = k_2'K$ (see text).

Scheme 2

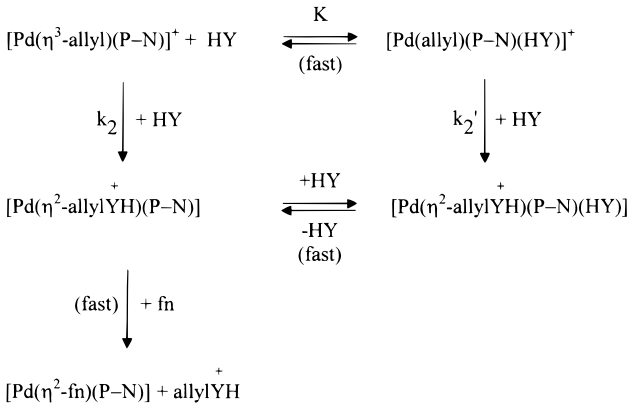

In light of ^{1}H NMR data we propose the mechanism of Scheme 2, where the cationic substrate undergoes nucleophilic attack by the entering amine at the allyl ligand (step k_2) or at the central metal (fast equilibrium K), forming the intermediate [Pd(allyl)(P−N)(HY)]$^+$ in which the allyl moiety is attacked by a further amine molecule (step k_2'). Although such an intermediate could not be detected in any ^{1}H NMR spectrum of the reaction mixtures, its formation (in low concentration) is suggested by the rate increase for both the $\eta^3{-}\eta^1{-}\eta^3$ and **II** ↔ **III** processes in the presence of the amine HY. Accordingly, the intermediate may be conceived of as a labile five-coordinate transient in equilibrium with an η^3-allyl species containing a P-monodentate iminophos-

(19) (a) Åkermark, B.; Vitagliano, A. *Organometallics* **1985**, *4*, 1275. (b) Åkermark, B.; Zetterberg, K.; Hansson, S.; Krakenberger, B.; Vitagliano, A. *J. Organomet. Chem.* **1987**, *335*, 133.

(20) Vitagliano, A.; Åkermark, B. *J. Organomet. Chem.* **1988**, *349*, C22.

Downloaded by CARLI CONSORTIUM on June 30, 2009
Published on February 27, 1999 on http://pubs.acs.org | doi: 10.1021/om980858l

phine ligand and/or with an η^1-allyl species containing a bidentate iminophosphine ligand. The k_2 and k_2' steps yield palladium(0) products with an η^2-bound allylammonium group, which are rapidly converted to the final derivative [Pd(η^2-fn)(P−N)] by the more π-accepting fumaronitrile ligand.

According to this mechanism, the rate law should be

$$k_{obs} = \frac{k_2[HY] + k_2'K[HY]^2}{1 + K[HY]} \qquad (5)$$

which reduces to eq 3 with $k_2'K = k_3$ if the term K[HY] is much lower than 1, as is expected from the inability to detect appreciable concentrations of the intermediate [Pd(allyl)(P−N)(HY)]$^+$. In this context the observed rate law 4 is a particular case of eq 3 when $k_2'K[HY] \ll k_2$.

Table 5 shows that the k_2 term increases with increasing basicity and decreasing steric demands of the amine, in agreement with our previous kinetic studies.[7,8] A marked decrease is observed on going from η^3-propenyl complexes **1a**−**4a** to the corresponding η^3-3-methyl-2-butenyl derivatives **1b**, **3b**, and **4b**, as a result of increased steric hindrance and decreased electrophilic character of the allyl fragment brought about by the methyl substituents.

A notable influence on k_2 is also exerted by the imino nitrogen substituent R of the P−N ligand. As can be seen in Table 5, the k_2 term increases with increasing electron-withdrawing ability of R: *cf.* **1a** (R = C_6H_4OMe-4) vs **2a** (R = Me). Surprisingly, with the bulkier and more electron donating CMe_3 and (*R*)-bornyl groups (**3a** and **4a**, respectively) higher k_2 values are observed. A similar effect is detected on going from **1b** to **3b** and **4b**. These findings can be rationalized by invoking some sort of distortion of the η^3-bound allyl ligand in the substrates **3a**, **3b** and **4a**, **4b**, which leads to an early, product-like transition state with marked allyl carbon reactivity. This ground-state allylic distortion is purported to play a major role in palladium-catalyzed asymmetric allylic aminations.[4c,21] Such interpretation is further supported by the marked distortion of the allylic ligand observed in the solid-state structure of complex **4b**(ClO_4) (*vide supra*). Accordingly, the amination rates of complexes [Pd(η^3-allyl)(L−L′)]$^+$ (L−L′ = 2-(thiomethyl)pyridine) were found to increase with increasing bulkiness of the pyridine group.[7]

When the k_2 data gathered so far for allyl amination of complexes [Pd(η^3-C_3H_5)(L−L′)]$^+$ by diethylamine, piperidine, and morpholine are compared, the following ranges are observed: L−L′ = 2-(iminomethyl)pyridine (N−N′), 1.2×10^{-2}−0.4;[8] iminophosphine (P−N), 3.2×10^{-2}−3.9 (this work); 2-(thiomethyl)pyridine (N−S), 0.2−10.0 mol^{-1} dm^3 s^{-1}. [7] These values correspond to the following gross reactivity order of L−L′: N−S > P−N > N−N′. It is noteworthy that replacement of a pyridine group in N−N′ by a tertiary phosphine group in P−N does not bring about any outstanding increase in the k_2 term, at variance with what expected from the higher *trans* influence of the phosphine group, which should render the allylic carbon *trans* to P more susceptible to nucleophilic attack.[11] The modest increase of the k_2 values on going from the N−N′ to the P−N complexes suggests that the nucleophilic attack on **1a**−**4a** may occur at both terminal allylic carbons (*i.e.*, *trans* to P and *trans* to N) unless one of the two carbons is preferentially attacked on steric grounds. Therefore, the k_2 values in Table 5 should be considered as the sum of the two contributions for **1a**−**3a**, while for **4a** each diastereoisomer will contribute to the experimental overall value. Moreover, due allowance being made for the different structural features of the P−N ligands, the selectivity in the nucleophilic attack at the allylic carbon *trans* to P, observed in the palladium-catalyzed asymmetric allylic amination with chiral ferrocenyl pyrazole−phosphine ligands,[4c] is likely to be caused by steric rather than electronic factors.

On the other hand, the higher reaction rates observed for **1a**−**4a** compared to those for complexes [Pd(η^3-C_3H_5)(N−N′)]$^+$ are mainly due to the lack of displacement of the P−N ligands by the secondary amines that we have used in this work. In fact, in the reactions of complexes [Pd(η^3-C_3H_5)(N−N′)]$^+$ the allylic amination is accompanied by reversible displacement of the N−N′ ligand by amines:[8]

$$[Pd(\eta^3\text{-}C_3H_5)(N{-}N')]^+ + 2HY \overset{K_E}{\rightleftharpoons} [Pd(\eta^3\text{-}C_3H_5)(HY)_2]^+ + N{-}N' \qquad (6)$$

Accordingly, the following experimental rate law was observed:

$$k_{obs} = \frac{k_2[HY] + k_3[HY]^2}{1 + K_E\dfrac{[HY]^2}{[N{-}N']}} \qquad (7)$$

where the ratio $1/(1 + K_E[HY]^2/[N{-}N'])$ represents the fraction of starting substrate that is reactive toward the amination, the bis(amine) displacement product [Pd(η^3-C_3H_5)(HY)$_2$]$^+$ being unreactive.[8]

For complexes **1b** and **3b**, for which the isomer ratio **II**/**III** remains constant throughout the reaction, the nucleophilic attack by diethylamine may take place at the unsubstituted allyl carbon of both isomers, at rates lower than that of interconversion. Thus, the observed k_2 values are again to be considered as the sum of the two contributions, unless one isomer is by far preferred for steric reasons. For **4b** the contribution to the experimental k_2 value is even more complicated by the presence of two diastereoisomers for each structure of types **II** and **III**. On the other hand, the k_2 values for the reaction of **1b**, **3b**, and **4b** with piperidine should be taken as merely indicative, since the amination occurs at both allyl carbon termini for each isomeric species of the substrate and is further complicated by isomerization of the allylamine products.

On the basis of the proposed mechanism, the quadratic k_3 term is the product of the equilibrium constant K and the second-order rate constant k_2'. Provided the K values are low, detection of the k_3 term for the η^3-propenyl complexes **1a**−**4a** implies in any case high values for k_2'. The enhanced reactivity of the intermediate [Pd(allyl)(P−N)(HY)]$^+$ may arise from a markedly distorted allyl group in a five-coordinate species. In this context, the absence of the quadratic k_3 term in the reactions of **1b**, **3b**, and **4b** could be explained by a

(21) Blöchl, P. E.; Togni, A. *Organometallics* **1996**, *15*, 4125.

Downloaded by CARLI CONSORTIUM on June 30, 2009
Published on February 27, 1999 on http://pubs.acs.org | doi: 10.1021/om980858l

Table 6. Elemental Analysis Data (%)[a]

complex	C	H	N
1b(BF_4)	56.8 (56.60)	4.7 (4.75)	2.1 (2.13)
2b(BF_4)	53.2 (53.08)	4.9 (4.81)	2.4 (2.48)
3b(BF_4)	55.1 (55.33)	5.6 (5.47)	2.2 (2.30)
4b(BF_4)	59.5 (59.36)	6.1 (6.01)	2.1 (2.04)

[a] Calculated values in parentheses.

considerable decrease in the k_2' values, which parallels the corresponding decrease observed for k_2 values.

Experimental Section

Materials. The iminophosphines,[10] the dimers [Pd(μ-Cl)(η^3-allyl)]$_2$ (allyl = C_3H_5 and 1,1-$Me_2C_3H_3$),[22] and the complexes **1a**(BF_4)−**4a**(BF_4)[10] were prepared by published methods. All other chemicals were commercial grade and were purified or dried by standard methods, when required.[23] The complexes **1b**(BF_4)−**4b**(BF_4) were prepared from the reaction of [Pd(μ-Cl)(η^3-1,1-$Me_2C_3H_3$)]$_2$ (0.25 mmol) with the appropriate iminophosphine P−N (0.5 mmol) in CH_2Cl_2 (20 mL), followed by addition of an excess of $NaBF_4$ (2 mmol) dissolved in 10 mL of methanol. The reaction mixture was worked up as previously described for **1a**(BF_4)−**4a**(BF_4),[10] to give the required products (yields in the range 68−87%, based on the theoretical amount), which were purified by reprecipitation from a CH_2Cl_2/Et_2O solvent mixture. Because of the straightforward method of preparation, the cationic complexes can be completely characterized by their multinuclear NMR spectral data. However, elemental analysis, IR spectra in the solid state, and molar conductivity measurements were also carried out in order to ascertain the composition, the presence of the BF_4^- anion (ν(B−F) around 1060 cm^{-1}), and the nature of uni-univalent electrolytes (molar conductivities in the range 91−98 Ω^{-1} cm^2 mol^{-1} for 1 × 10^{-3} mol L^{-1} MeOH solutions at 25 °C). The elemental analysis data of the η^3-2-methyl-2-propenyl complexes are given in Table 6. The complex **4b**(ClO_4) was prepared similarly, using $NaClO_4 \cdot H_2O$ instead of $NaBF_4$ (yield 90%). The ^1H and ^{31}P NMR spectra of **4b**(ClO_4) were found to be identical with those of **4b**(BF_4). Clear, yellow crystals of **4b**(ClO_4) suitable for X-ray analysis were obtained by slow diffusion of diethyl ether into a dilute dichloromethane solution.

NMR Measurements. The ^1H,$^{13}C\{^1H\}$, and $^{31}P\{^1H\}$ NMR spectra were recorded on a Bruker AM 400 spectrometer, operating at 400.13, 100.61, and 161.98 MHz, respectively. Chemical shifts (ppm) are given relative to Me_4Si (^1H and ^{13}C NMR) and 85% H_3PO_4 (^{31}P NMR). The amination reactions were monitored by recording ^1H NMR spectral changes of $CDCl_3$ solutions, prepared by dissolving 0.05 mmol of the allyl complex and the appropriate amounts of amine and fumaronitrile in 2 mL of the solvent. The ^1H 2D ROESY spectrum of **2b**(BF_4) in $CDCl_3$ was obtained in the phase-sensitive mode using the TPPI phase cycle with the ROESY pulse sequence, modified to eliminate the offset dependence of cross-peak intensity.[24] A total of 128 transients on a size of 2K were accumulated in the phase-sensitive mode for 512 experiments. A spin-lock period corresponding to a transverse mixing time of 0.3 s was applied. Data were processed with the 2D NMR program TRITON, licensed by the University of Utrecht, Utrecht, The Netherlands. Elaboration of the spectrum was carried out on a Digital Graphic workstation. A sine bell apodization function, shifted by $\pi/3$, was applied in both dimensions. A zero filling was applied in t1 in order to obtain a real 1K × 1K matrix.

Table 7. Crystal Data and Details of Data Collection for 4b(ClO_4)

formula	$C_{34}H_{41}ClNO_4PPd$	T (°C)	25(2)
space group	*P*1	λ (Å)	0.710 73
cryst syst	triclinic	*Z*	2
fw	700.5	*F*(000)	724
a (Å)	10.460(6)	*V* (Å^3)	1632(1)
b (Å)	10.938(5)	D_{calcd} (g/cm^3)	1.426
c (Å)	15.785(7)	μ (cm^{-1})	7.37
α (deg)	97.05(4)	*R*[a]	0.041
β (deg)	107.15(4)	R_w[a]	0.104
γ (deg)	104.58(4)	GOF[b]	1.053

[a] $R = \sum(||F_o| - |F_c||)/\sum(|F_o|)$; $R_w = [\sum[w(|F_o|^2 - |F_c|^2)]^2/\sum(w|F_o|^2)^2]^{1/2}$. [b] GOF = $[\sum w(|F_o|^2 - |F_c|^2)^2/(N_{obs} - N_{par})]^{1/2}$.

X-ray Structural Analysis of 4b(ClO_4). Intensity data were collected on a Siemens Nicolet R3m/V diffractometer using the $\omega-2\theta$ scan mode. The unit cell was determined by the automatic indexing of 50 centered reflections. Crystal decay was negligible, and correction was deemed unnecessary, while an empirical absorption correction based on Ψ-scans was applied (T_{max} = 0.951, T_{min} = 0.356). A total of 5155 reflections were collected in the range $4 < 2\theta < 48°$, of which 4722 reflections with $I > 2\sigma(I)$ were used for the structure determination. The structure was solved by the Patterson method using SHELXTL/PC[25] and refined by the full-matrix least-squares method on F^2 using SHELXL-93.[26] All non-hydrogen atoms were refined anisotropically, and the positions of the hydrogen atoms were located geometrically and constrained to ride on the carbon atoms to which they are bonded with their thermal parameters fixed at values of 1.2 or 1.5 (for methyl groups) of their parent atoms. Their contributions were added to the structure factor calculations, but their positions were not refined. The chirality was defined from the Flack coefficient, 0.03(4).[27] The final difference map was featureless, apart from some peaks (up to 0.888 e Å^{-3}) in the vicinity of the ClO_4^- tetrahedrons. The crystal data and details of data collection are listed in Table 7.

Kinetic Measurements. The kinetics of allyl amination were studied by addition of known aliquots of amine solution to a solution of the complex under study and fumaronitrile in the thermostated cell compartment of a Perkin-Elmer Lambda 40 spectrophotometer (25 °C). Mathematical and statistical data analysis was carried out on a personal computer by means of a locally adapted version of Marquardt's algorithm written in TURBOBASIC (Borland).[28]

Acknowledgment. Financial support by the Italian Ministero per l'Università e la Ricerca Scientifica e Tecnologica is gratefully aknowledged.

Supporting Information Available: Tables of complete crystallographic experimental details, positional parameters for all atoms, bond distances and angles, anisotropic thermal parameters, and hydrogen atom coordinates. This material is available free of charge via the Internet at http://pubs.acs.org.

OM980858L

(22) (a) Hartley, F. R.; Jones, S. R. *J. Organomet. Chem*. **1974**, *66*, 469. (b) Powell, J.; Shaw, B. L. *J. Chem. Soc. A* **1967**, 1839.
(23) Armarego, W. L. F.; Perrin, D. D. *Purification of Laboratory Chemicals*, 3rd ed.; Pergamon Press: NewYork, 1988.
(24) (a) Marion, D.; Wuthrich, K. *Biochem. Biophys. Res. Commun*. **1983**, *113*, 964. (b) Bothner-By, A. A.; Stephens, R. L.; Lee, J.; Warren, C. D.; Jeanloz, R. W. *J. Am. Chem. Soc*. **1984**, *105*, 811. (c) Griesinger, C.; Ernst, R. R. *J. Magn. Reson*. **1987**, *75*, 261.
(25) Sheldrick, G. M. SHELXTL/PC Version 5.03; Siemens Analytical X-ray Instruments Inc., Madison, WI, 1994.
(26) Sheldrick, G. M. SHELX-93; University of Gottingen, Gottingen, Germany, 1993.
(27) Flack, H. D. *Acta Crystallogr*. **1983**, *A39*, 876.
(28) Marquardt, D. W. *SIAM J. Appl. Math*. **1963**, *11*, 431.
(29) We thank Prof. P. S. Pregosin for this suggestion.